

The Kelvin Waves in Vortex Dynamics and Their Stability

JACOB BURBEA*

*Department of Mathematics, University of Pittsburgh, Pittsburgh,
Pennsylvania 15260*

AND

MICHAEL LANDAU

*PPG Industries, Inc., Fiber Glass Research Center, P.O. Box 2844,
Pittsburgh, Pennsylvania 15230*

Received April 28, 1981

The rotating m -waves of Kelvin form a class \mathcal{K}_m , $m \geq 2$, of m -fold symmetric regions D of constant vorticity $\omega_0 \equiv 1$ which are uniformly rotating with an angular velocity (bifurcation parameter) Ω in the range $\Omega_{m-1} < \Omega \leq \Omega_m$, $\Omega_m \equiv (m-1)/2m$. The class \mathcal{K}_2 corresponds to the rotating ellipses of Kirchoff. We present a numerical method for the determination of the stability-characteristics of the class \mathcal{K}_m . The method, based on Burbea's theory of the stability of vortex-motions, uses conformal mappings to construct the spectrum of a certain crucial "stability-operator" B . Numerical results show the existence of a critical value $\Omega_{cr}(m) = (3\Omega_m + \Omega_{m-1})/4$ with the following property: Given any $\Omega \in (\Omega_{m-1}, \Omega_m]$, there exists a steady state $D \in \mathcal{K}_m$, unique up to a rotation, magnification and reflection, whose angular velocity is Ω . Moreover, this state is (secularly) stable if and only if $\Omega_{cr}(m) < \Omega \leq \Omega_m$. Other stability-characteristics of the class \mathcal{K}_m are determined. The entire results of Love for the particular class \mathcal{K}_2 are obtained here as special cases.

1. INTRODUCTION

Recent analytical and computational work in two-dimensional vortex-dynamics establishes the existence of certain periodical steady states of vortex motions (Burbea [1, 3], Deem and Zabusky [5], Landau [11], Landau and Zabusky [12], Pierrehumbert [14] and Saffman and Szeto [15]). A convenient way of expressing these states is via the conformal mapping ϕ of the exterior of the circle onto the exterior of a region D (vortex) of vorticity ω [1], in general assumed to be a constant $\omega \equiv \omega_0$. The boundary ∂D of a steady vortex D is then a streamline for an incompressible flow with a stream function ψ and such that ∂D forms the boundary of discontinuity of the vorticity-function $\Delta\psi$. In that case $\Delta\psi = \omega_0 - 2\Omega$ in the interior of D while $\Delta\psi = -2\Omega$ in its exterior, where the constant Ω serves as a (major) bifurcation parameter, representing the angular velocity of the vortex D about its centroid (assumed to be at the origin).

*This research was completed while this author was visiting the Mittag-Leffler Institute, Sweden, during 1981-1982.

When the vortex D is a single simply connected region which is subject to only uniform rotation, the resulting steady states themselves tend to be rigidly rotating. In 1880 Kelvin showed that small perturbation of the circle proportional to $\cos m\theta$ rotated uniformly with angular velocity $\Omega = (1/2) \omega_0(m-1)/m$, $m \geq 2$ (see Lamb [10, p. 231]). Another well-known (exact) steady state is the elliptical vortex of Kirchoff [10, p. 232] with the angular velocity $\Omega = \omega_0 Q/(1+Q)^2$, where Q is the aspect-ratio of the ellipse (i.e., the ratio of the minor radius over the major radius), $Q \in (0, 1]$. This rotating ellipse is the finite amplitude form of the $m=2$ wave of Kelvin. We shall refer to the finite amplitude form of the m -waves of Kelvin as the class \mathcal{K}_m , $m \geq 2$, of the Kelvin waves.

The problem of finding the shapes of the steady states D in the class \mathcal{K}_m , $m \geq 3$, and their angular velocities was recently attacked numerically by Deem and Zabusky [5]. They showed two examples of steady states in the class \mathcal{K}_m for $m=3, 4$, all valid to three significant figures. The computations in [5] were done by employing a "contour-dynamics" algorithm. In Burbea [1], a proof for the existence of these Kelvin waves was given by bifurcating the trivial solution of the circle. Moreover, an analytical method, based on asymptotic expansion of conformal mappings, for the determination of the states $D \in \mathcal{K}_m$ and their angular velocities was presented (Burbea [3]). These steady states are m -fold symmetric regions of constant vorticity and are uniformly rotating. They constitute a generalization of the rotating ellipse of Kirchoff which corresponds to $m=2$.

Once a steady vortex is found, the question of its stability-characteristics presents itself naturally. In 1898, Love [13] gave a complete account of the stability properties of the entire elliptic class \mathcal{K}_2 . This was done by deforming the elliptic vortex $D \in \mathcal{K}_2$ with a perturbation field which is irrotational everywhere. The stability analysis in Love [13] was accomplished by appealing to classical methods of matching, on the boundary of the disturbed elliptical vortex, the exterior and interior stream functions, and, following the tradition established by Kirchoff, Love used cartesian coordinates to describe the interior of the elliptic vortex while elliptical coordinates were used to describe its exterior. In this way a simple, but nevertheless ingenious, analysis was possible. However, in spite of the ingenious ingredients of Love's method, his analysis seems to be applicable only in the case where the vortex is elliptical.

It is rather surprising that since Love's work no explicit stability-characteristics of vortex motions which are not elliptic seems to have appeared in the literature. In this regard, no exception is made for the existing Kelvin's variational principle on the excess-energy for the steady vortex motions (see, for example, [15]). Needed in a stability-characteristics are the following ingredients: (1) an explicit and precise perturbation field $\mathcal{F}(D)$ for the steady state D , (2) an effective stability-criterion for the steady vortex in terms of the spectrum of a relevant operator B whose domain of definition is $\mathcal{F}(D)$, (3) an explicit rule which orders the eigenvalues and eigenvectors of B as natural modes and harmonics and, finally, (4) an explicit dispersion-relation for the perturbation of the steady vortex in terms of the natural modes of B .

Such a stability-characteristics has recently been presented in Burbea [2, 4] when

the steady vortex D is a single simply-connected region of constant vorticity ω_0 and is subjected to rotation and strains of any order. It is an effective and coordinate-free stability condition, applicable to a more general family of steady states which contains the m -Kelvin waves \mathcal{K}_m as a subfamily. In particular, with this stability-characteristics the results of Love [13], on the stability of class \mathcal{K}_2 , are obtained as special cases. The stability-criterion that is provided in Burbea [2, 4] is formulated in terms of the spectrum of a self-adjoint operator B in the space of complex sequences l_2 . This "stability-operator" is an elementary expression involving the so called "Grunsky," "Hankel" and "Toeplitz" operators, G , H and T , respectively, of the steady vortex D . These important operators introduced in Burbea [2, 4], embody the relevant information concerning the boundary of the steady vortex D as the normal derivative of the stream function and the condition for non-singularity of the vortex. The actual expression for the stability-operator B is

$$B = \left(\frac{\omega_0}{2}\right)^2 [(I - T)^2 - (G - H)(\bar{G} - \bar{H})],$$

where I is the identity operator on l_2 and the bar denotes complex conjugation.

In this paper we give a detailed stability analysis of the m -Kelvin waves \mathcal{K}_m for $m \geq 3$. In particular, we shall compute the critical values of the angular velocity $\Omega_{cr}(m)$ and of the aspect-ratio $Q_{cr}(m)$ for the stability of any steady vortex $D \in \mathcal{K}_m$. Moreover, we give an exhaustive account of the stability properties of any class \mathcal{K}_m in such a way that the entire results of Love [13] for the elliptic case \mathcal{K}_2 will appear as special cases. To do so we must, of course, compute first the steady states of \mathcal{K}_m and their corresponding angular velocities. This may be accomplished by analytical methods described in Burbea [3]. We, however, proceed in a different, but numerically more direct, manner described below.

The steady vortex $D \in \mathcal{K}_m$ and its angular velocity Ω are determined by a first-order relaxation algorithm, developed first in Landau [11] (see also Landau and Zabusky [12]) and is similar to that of Pierrehumbert [14] in the two singly-connected case. Once $D \in \mathcal{K}_m$ is determined, we numerically compute the conformal mapping ϕ of the exterior of the unit disk onto the exterior of D . This will be accomplished via the Theodorsen method (Gaier [6]) and thereby the Grunsky-operator G is determined. The Hankel- and the Toeplitz-operators H and T , respectively, will be determined by computing the normal derivative of the stream function ψ along the boundary of D , parametrized by the conformal mapping ϕ . We then form the crucial stability-operator B . The spectrum of the truncation of this operator will be determined by a QR -algorithm [16] whence the natural modes and the dispersion-relation of the perturbation of $D \in \mathcal{K}_m$ are obtained. The stability analysis is concluded with the investigation of the positivity of the spectrum along with other stability-characteristics.

In Section 2 we give a brief account of the theoretical ingredients, based on Burbea [2, 4], and, we formulate the rules of the stability-characteristics for steady vortex motions. Section 3 is a preliminary discussion of the properties of the Kelvin waves

\mathcal{K}_m from the analytical standpoint. It serves as a guide and a motivation for our numerical findings as well as a test to the efficacy of the general theory of Section 2. In Section 4 we describe in detail the actual numerical algorithm and give flow-charts for the code itself. Section 5 is a report on our numerical findings. It constitutes a summary of the properties of Kelvin waves \mathcal{K}_m and their stability-characteristics.

As an illustration of the scope of the new findings we wish to single out the following result, stated in terms of dimensionless quantities with $\omega_0 \equiv 1$:

Given any integer $m \geq 2$ and any number Ω in the range

$$\frac{1}{2} \frac{m-2}{m-1} < \Omega \leq \frac{1}{2} \frac{m-1}{m},$$

there exists a steady (m -fold symmetric) vortex $D \in \mathcal{K}_m$, unique up to rotation, magnification and reflection, whose angular velocity is Ω . This steady vortex is (secularly) stable if and only if $\Omega > \Omega_{\text{cr}}(m)$, where

$$\Omega_{\text{cr}}(m) = \frac{1}{8} \left(3 \frac{m-1}{m} + \frac{m-2}{m-1} \right).$$

2. GENERAL THEORY

We give a brief account of the theoretical tools needed in this work and we refer the reader to the works of Burbea [1-4] for analytical details and extensions.

Under consideration is a two-dimensional incompressible flow $\mathbf{u} = (-\partial_y \psi, \partial_x \psi)$ with a stream function ψ . The vorticity of the flow $\Delta \psi$, in consistency with the Euler-equation, is chosen to be a piecewise constant. By a vortex we mean a compact subset D of the plane whose boundary $C = \partial D$ is a boundary of discontinuity of the vorticity $\Delta \psi$. For simplicity, we shall assume that the vortex D is a single Jordan region whose boundary C is sufficiently smooth. The vorticity is chosen to be $\omega_0 - 2\Omega$ in D and -2Ω in the exterior E_D of D . Here, ω_0 is a given constant while the angular velocity Ω of D about its centroid serves as a (major) bifurcation parameter.

As in [1-4], it is found very convenient to employ complex notation. Accordingly, for $z = x + iy$ we use

$$\partial_z = \frac{1}{2}(\partial_x - i\partial_y), \quad \partial_{\bar{z}} = \frac{1}{2}(\partial_x + i\partial_y)$$

and thus $\Delta = 4\partial_z \partial_{\bar{z}}$, and, $\mathbf{u} = 2i\partial_{\bar{z}}\psi$. The area Lebesgue measure is denoted by $d\sigma(z) = dx dy$. Under these circumstances the stream function ψ may be given by

$$\psi(z) = \frac{\omega_0}{2\pi} \int_D \log |\zeta - z| d\sigma(\zeta) + R(z) \quad (2.1)$$

with

$$R(z) = -\frac{1}{2}\Omega |z|^2 + \operatorname{Re} L(z), \quad (2.2)$$

where $L(z)$ is an entire-holomorphic function. In the case of the m -waves of Kelvin, $L(z)$ is chosen to be identically zero. The boundary of the vortex is convected with the flow, and thus the flow is wholly tangential. Mathematically, this becomes

$$2 \operatorname{Re}[z' \partial_z \psi] = \operatorname{Re}[z' i \dot{z}], \quad z \in C, \quad (2.3)$$

as a condition for the boundary C . Here, $z = z(s, t)$ is the parametric representation of C with respect to the arc-length s and time t , and, a prime and a dot denote differentiation with respect to s and t , respectively.

Equation (2.3), together with (2.1)–(2.2), is the evolution equation for the boundary C of the vortex. A steady solution of this equation satisfies $\partial_s \psi = 0$ which is equivalent to

$$2z' \partial_z \psi = i \partial_n \psi; \quad z = z(s) \in C, \quad (2.4)$$

where $\partial_n \psi$ is the normal derivative of the stream function. This means that C is a streamline for ψ .

Once a steady solution D is found, the conformal mapping $z = g(\omega)$ which maps the exterior of the unit disk $E_\Delta = \{\omega: |\omega| > 1\}$ onto the exterior of the vortex E_D can be determined. The mapping $g(\omega)$ is always of the form

$$g(\omega) = a\phi(\omega), \quad \phi(\omega) = \omega + \sum_{n=0}^{\infty} b_n \omega^{-n}, \quad a \neq 0; \omega \in E_\Delta. \quad (2.5)$$

The *Grunsky-coefficients* b_{nk} of ϕ are defined by

$$\log \frac{\phi(\omega) - \phi(\tau)}{\omega - \tau} = - \sum_{n,k=1}^{\infty} b_{nk} \omega^{-n} \tau^{-k}; \quad \omega, \tau \in E_\Delta. \quad (2.6)$$

These coefficients form a symmetric matrix with $b_{n1} = b_{1n}$, $n \geq 1$ and the recursion formula

$$(n+1) b_{n+1,k} = b_{n+k} + n b_{n,k+1} + n \sum_{j=1}^{k-1} b_{k-j} b_{nj} - \sum_{j=1}^{n-1} j b_{n-j} b_{jk}. \quad (2.7)$$

We consider the customary complex Hilbert space l_2 of sequences $\alpha = (\alpha_1, \alpha_2, \dots)$ with the inner product and norm

$$(\alpha, \beta) = \sum_{n=1}^{\infty} \alpha_n \bar{\beta}_n, \quad \|\alpha\| = \sqrt{(\alpha, \alpha)}.$$

Let A be a linear operator in l_2 with a matrix representation $A = (A_{nk})$ and whose domain of definition \mathcal{D}_A is dense in l_2 . We define $\bar{A} = (\bar{A}_{nk})$ and $A^t = (A_{kn})$ to be the matrix transpose of A (note that $\mathcal{D}_{\bar{A}} = \mathcal{D}_A$). The adjoint of A is given by $A^* = \bar{A}^t$. The operator A is self-adjoint if $A^* = A$ and is symmetric if $A^* = \bar{A}$.

The Grunsky-operator $G = (G_{nk})$ is defined by $G_{nk} = \sqrt{nk} \bar{b}_{nk}$, where the b_{nk} are the Grunsky-coefficients of the mapping ϕ of (2.6). This is a symmetric operator in l_2 which is also bounded with norm $\|G\| \leq 1$. Moreover, $\|G\| < \kappa$ for some $0 \leq \kappa < 1$ if and only if the boundary of the vortex D has no cusps.

Referring now to (2.4) and (2.5) we define the *vortex-function*

$$r(\theta) = \frac{2}{\omega_0} \frac{1}{|g'(e^{i\theta})|} \partial_n \psi [g(e^{i\theta})], \quad \theta \in [0, 2\pi]. \quad (2.8)$$

Since $\partial_n \psi$ is a real-valued continuous function on C it follows that $r(\theta)$ is real-valued and continuous in $\theta \in [0, 2\pi]$. The Fourier expansion of $r(\theta)$ is, therefore,

$$r(\theta) = \sum_{n=-\infty}^{\infty} r_n e^{in\theta}; \quad r_{-n} = \bar{r}_n. \quad (2.9)$$

Associated with this vortex-function are the *Hankel-* and *Toeplitz-operators* $H = (H_{nk})$ and $T = (T_{nk})$, respectively. They are defined by $H_{nk} = \sqrt{nk} r_{n+k}$ and $T_{nk} = \sqrt{nk} r_{n-k}$, where it is stipulated that their common domain of definition \mathcal{D} is dense in l_2 . Evidently, H is symmetric and T is self-adjoint in l_2 .

With the aid of the operators G , H and T we introduce the crucial *stability-operator*

$$B = \left(\frac{\omega_0}{2}\right)^2 [(I - T)^2 - (G - H)(\bar{G} - \bar{H})], \quad (2.10)$$

where I is the identity operator in l_2 . This operator is self-adjoint in l_2 with \mathcal{D} as its domain of definition. We also introduce the *companion-operator*

$$J = \left(\frac{\omega_0}{2}\right)^2 [(G - H)\bar{T} - T(G - H)] \quad (2.11)$$

whose domain of definition is also \mathcal{D} and is skew-symmetric in l_2 , i.e., $J^* = -\bar{J}$.

In order to investigate the stability of the steady vortex D , the evolution equation (2.3) should be linearized about this steady state with a perturbation field which is anti-holomorphic in D . This leads to the following stability-characteristics enunciated and first proved in Burbea [2, 4]:

STABILITY-CHARACTERISTICS. Let $z = g(e^{i\theta}) = a\phi(e^{i\theta})$, as in (2.5), describe the boundary of the steady vortex D . Then, the following hold:

(1) *Stability-Criterion.* The vortex is stable (with respect to $\mathcal{D} \subset l_2$) if and only if B is a positive operator, i.e., the quadratic form $(B\alpha, \alpha)$ is positive-definite for $\alpha \in \mathcal{D}$, $\alpha \neq 0$.

(2) *Stability-Test.* $(J\bar{\alpha}, \alpha) = 0$ for every $\alpha \in \mathcal{D}$ and in order that the vortex be stable (with respect to \mathcal{D}) it is necessary that $\bar{J}\alpha = 0$ for $\alpha \in \mathcal{D}$.

(3) *Natural-Modes.* The eigenvalues (necessarily real) σ^2 and the corresponding eigenvectors α of B are ordered as natural-modes by the following rule: the n -mode $\alpha^{(n)}$ is the eigenvector α of B so that the eigenfunction

$$F_\alpha(\theta) \equiv \frac{1}{|g'(e^{i\theta})|^2} \operatorname{Re} [g'(e^{i\theta}) \overline{P(e^{i\theta})}]$$

with

$$P(e^{i\theta}) = \sum_{k=1}^{\infty} \alpha_k k^{1/2} e^{i(k-1)\theta}, \quad \alpha = (\alpha_1, \alpha_2, \dots),$$

has $2(n-1)$ zeros in $[0, 2\pi]$. The natural n -eigenvalue σ_n^2 is the eigenvalue of B corresponding to the n -mode $\alpha^{(n)}$. The natural n -harmonic is the (natural) n -eigenfunction

$$F_n(\theta) \equiv F_{\alpha^{(n)}}(\theta).$$

(4) *Dispersion-Relation.* The dispersion-relation of the perturbation of the vortex is determined by

$$\sigma_n^2 = (B\alpha^{(n)}, \alpha^{(n)}) / \|\alpha^{(n)}\|^2$$

or

$$\sigma_n^2 = \left(\frac{\omega_0}{2}\right)^2 \{ \|(I - T)\alpha^{(n)}\|^2 - \|(\bar{G} - \bar{H})\alpha^{(n)}\|^2 \} / \|\alpha^{(n)}\|^2,$$

and, therefore, the vortex is n -mode stable if and only if $\sigma_n^2 > 0$.

When the steady vortex D is symmetric about the real axis, the above formulation may be simplified as follows: First, the coefficients b_n of the mapping in (2.5) are all real and, therefore, the Grunsky-coefficients b_{nk} in (2.6) are also all real. Moreover, the coefficients r_n of (2.9) are real, that is, $r_{-n} = r_n$ and, therefore

$$r(\theta) = r_0 + 2 \sum_{n=1}^{\infty} r_n \cos n\theta. \quad (2.12)$$

It therefore follows that the Grunsky-, Hankel- and Toeplitz-operators are all real symmetric matrix-operators. This shows that the stability-operator B in (2.10) is now the real symmetric operator

$$B = \left(\frac{\omega_0}{2}\right)^2 [(I - T)^2 - (G - H)^2] \quad (2.13)$$

while the companion-operator J in (2.11) is now the real-skew symmetric operator

$$J = \left(\frac{\omega_0}{2}\right)^2 [(G - H)T - T(G - H)]. \quad (2.14)$$

Moreover, the eigenvectors α of B all have real entries.

A further and significant simplification occurs when the steady vortex D is m -fold symmetric about the origin ($m \geq 2$). In this case the coefficients b_n in (2.5) are all zero except those for which $n + 1$ is a multiple of m , and thus

$$\phi(\omega) = \omega \left[1 + \sum_{n=1}^{\infty} b_{nm-1} \omega^{-nm} \right].$$

Moreover, the Grunsky-coefficients b_{nk} are all equal to zero if $n + k$ is not a multiple of m while for the non-zero coefficients the recursion formula (2.7) becomes

$$\begin{aligned} nb_{nk} = & b_{n+k-1} + (n-1)b_{n-1,k-1} + (n-1) \sum_{j=1}^{\lfloor k/m \rfloor} b_{jm-1} b_{n-1,k+1-jm} \\ & - \sum_{j=1}^{\lfloor (n-2)/m \rfloor} (n-jm) b_{jm-1} b_{n-jm,k}. \end{aligned} \quad (2.15)$$

Also, in (2.9) the coefficients r_n are zero if n is not a multiple of m and corresponding to (2.12) we now have

$$r(\theta) = r_0 + 2 \sum_{n=1}^{\infty} r_{nm} \cos nm\theta. \quad (2.16)$$

These simplifications are inherited by the operators G, H and T and therefore by B and J .

The uniformly rotating waves of Kelvin are obtained when the entire function $L(z)$ in (2.2) is chosen to be identically zero. These waves are m -fold symmetric steady states (Burbea [1, 3]), belonging to the Kelvin class \mathcal{K}_m , and, may always be normalized to be symmetric about the real-axis. In that case, an effective expression for the vortex function $r(\theta)$ in (2.8) may be obtained as follows: we let $z = x + iy = g(e^{i\theta}) \in C$ with $x = x(\theta)$, $y = y(\theta)$, and, denoting differentiation with respect to θ by a dot, we have

$$r(\theta) = \frac{2}{\omega_0} \frac{1}{x^2 + y^2} (y\dot{x}\psi - x\dot{y}\psi) \quad (2.17)$$

with

$$\partial_x \psi = -\frac{\omega_0}{4\pi} \int_C \log |z - \zeta|^2 d\eta - \Omega x, \quad (2.18)$$

$$\partial_y \psi = \frac{\omega_0}{4\pi} \int_C \log |z - \zeta|^2 d\xi - \Omega y; \quad \zeta = \xi + i\eta \in C, \quad (2.19)$$

evaluated at $z = x + iy = g(e^{i\theta})$. Furthermore, the coefficients r_{nm} in (2.16) are now given by

$$r_{nm} = \frac{1}{2\pi\omega_0} \int_0^{2\pi} \frac{1}{x^2 + y^2} (\dot{y}\partial_x\psi - \dot{x}\partial_y\psi) \cos nm\theta d\theta; \quad n = 0, 1, 2, \dots \quad (2.20)$$

3. PROPERTIES OF KELVIN WAVES-PRELIMINARY (ANALYTICAL) REPORT

In this section we discuss the properties of the Kelvin waves \mathcal{K}_m from the analytical standpoint. As such this report is preliminary in nature. A conclusive numerical report based on the present general theory is given in Section 5.

It is convenient to deal with dimensionless quantities and this corresponds to taking $\omega_0 \equiv 1$. Besides the angular velocity Ω which serves as a (major) bifurcation parameter, it is also found convenient to introduce an auxiliary parameter μ by

$$\mu = 1 - 2\Omega. \quad (3.1)$$

The aspect-ratio Q , $Q \in (0, 1]$ of a Kelvin-vortex $D \in \mathcal{K}_m$ is directly related to its angular velocity Ω , and hence to μ . In general, however, this relationship is very involved (cf. Burbea [3]). With the natural n -eigenvalue σ_n^2 of the stability-operator B we consider the quantity

$$\lambda(n) \equiv \lambda(n; \Omega) = \sigma_n^2; \quad n = 1, 2, \dots, \quad (3.2)$$

which is also a (real-valued) function of μ or Q . Another quantity, playing a role in this work, is

$$\Omega_m \equiv \frac{1}{2} \frac{m-1}{m}, \quad m \geq 2.$$

In order to motivate our numerical findings we discuss first the situations where closed-form solutions can be found. This will also serve as a test to the efficacy of the previously described general theory. The present analysis follows the lines of Burbea [2, 4]. In (2.5), we take the mapping

$$\phi(e^{i\theta}) = e^{i\theta} + be^{-i\theta}, \quad 0 \leq |b| < 1, \quad (3.4)$$

describing an ellipse with aspect-ratio

$$Q = \frac{1 - |b|}{1 + |b|}. \quad (3.5)$$

It forms a steady rotating vortex if and only if

$$\bar{b}[\mu - 2^{-1}(1 + |b|^2)] = 0 \quad (3.6)$$

and in that case the vortex-function $r(\theta)$ is the constant $r(\theta) \equiv r_0$ satisfying

$$r_0 = \mu - |b|^2, \quad br_0 = b(1 - \mu) \quad (r_n = 0, n \geq 1). \quad (3.7)$$

The Grunsky-operator of (3.4) is the diagonal matrix $G = (\bar{b}^n \delta_{nk})$ and by (3.7) the Hankel-operator is $H = 0$ and the Toeplitz-operator is $T = r_0(n\delta_{nk})$. Consequently, the stability-operator is now the diagonal matrix

$$B = \frac{1}{4}[(1 - nr_0)^2 - |b|^{2n}] \delta_{nk}$$

while the companion-operator is now $J = 0$. Moreover, the n th diagonal element of B is precisely the natural n -eigenvalue σ_n^2 of B and the "Dispersion-Relation" (4) now reads

$$\lambda(n) = \sigma_n^2 = \frac{1}{4}[(1 - nr_0)^2 - |b|^{2n}]. \quad (3.8)$$

Equation (3.6) shows that the trivial circle-solution $b = 0$ is a steady vortex with μ being arbitrary. In this case, by (3.7), $r_0 = \mu$ and, therefore by (3.8)

$$\lambda(n) = \frac{1}{4}(n\mu - 1)^2, \quad n \geq 1 \quad (b = 0, \mu \text{ arbitrary}).$$

This solution is, therefore, stable for all modes $n \geq 1$, provided $\mu \neq m^{-1}$ where m is some integer $m \geq 1$. In the case that indeed $\mu = m^{-1}$ the solution whose angular velocity, in view of (3.1) and (3.3), is Ω_m is (secularly) stable with a dispersion-relation

$$\lambda_m(n; \Omega_m) = \frac{1}{4} \left(\frac{1}{m} n - 1 \right)^2; \quad n \geq 1, b = 0. \quad (3.9)$$

This forms the basis for the existence of the m -waves of Kelvin as solutions which bifurcate from the circle-solution $b = 0$ when the parameter μ of (3.1) takes on the value m^{-1} (cf. Burbea [1, 4]). The case of $m = 1$ is excluded for in that case, by (3.1), $\Omega = 0$. The corresponding auxiliary parameter μ of these m -waves lies in

$$m^{-1} \leq \mu < (m - 1)^{-1}, \quad m \geq 2. \quad (3.10)$$

It therefore follows that for any number μ satisfying (3.10) there exists a steady vortex $D \in \mathcal{X}_m$, unique up to a rotation, magnification and reflection, such that its angular velocity is $\Omega = (1 - \mu)/2$. In terms of Ω the range of existence of \mathcal{X}_m , in view of (3.1), (3.3) and (3.10), is

$$\Omega_{m-1} < \Omega \leq \Omega_m \quad (3.11)$$

and we note that the circle-solution is a member of every class \mathcal{X}_m with angular velocity $\Omega = \Omega_m$.

The class \mathcal{X}_2 is determined by (3.4)–(3.7) with $0 < |b| < 1$, giving

$$\mu = 2^{-1}(1 + |b|^2), \quad r_0 = 2^{-1}(1 - |b|^2); \quad 0 < |b| < 1 \quad (3.12)$$

and, therefore, using (3.1) and (3.5),

$$\Omega = \frac{1}{4} (1 - |b|^2) = \frac{Q}{(1 + Q)^2}. \quad (3.13)$$

This shows that \mathcal{X}_2 is identically the class of Kirchoff ellipses (Lamb [10, p. 232] and Love [13]) and we note that (3.11) and (3.13) are consistent. Moreover, from (3.8) and (3.12) we have

$$\lambda_2(n) \equiv \lambda_2(n; \Omega) = \frac{1}{4} \left\{ \left[\frac{n}{2} (1 - |b|^2) - 1 \right]^2 - |b|^{2n} \right\}, \quad 0 \leq |b| < 1, \quad (3.14)$$

which is consistent with (3.9) when $m = 2$ and $b = 0$. This dispersion-relation agrees with that of Love, which he obtained by using classical methods. In terms of the aspect-ratio Q or the angular velocity Ω , (3.14) reads

$$\lambda_2(n) = \frac{1}{4} \left\{ \left[2n \frac{Q}{(1 + Q)^2} - 1 \right]^2 - \left(\frac{1 - Q}{1 + Q} \right)^{2n} \right\}, \quad 0 < Q \leq 1, \quad (3.15)$$

or

$$\lambda_2(n) = \frac{1}{4} \{ (1 - 2n\Omega)^2 - (1 - 4\Omega)^n \}, \quad 0 < \Omega \leq 1/4. \quad (3.16)$$

The natural n -harmonic in the perturbation field of this elliptic-vortex (3.4) is

$$F_n(\theta) = \frac{n^{1/2}}{|\phi'(e^{i\theta})|^2} \operatorname{Re}[\phi'(e^{i\theta}) e^{-i(n-1)\theta}]$$

and we note that in consistency with the ‘‘Natural-Modes’’ (3) principle, $F_n(\theta)$ has $2(n - 1)$ zeros in $[0, 2\pi]$.

As already been noticed by Love [13], (3.15) shows that

$$\lambda_2(1) = \Omega^2, \quad \lambda_2(2) = 0 \quad (0 < Q \leq 1) \quad (3.17)$$

and $\lambda_2(3) > 0$ if and only if $Q > 3^{-1}$. This results in the existence of a critical aspect-ratio $Q_{cr}(2) \equiv 3^{-1}$ of the class \mathcal{X}_2 with the property that any (elliptic) vortex $D \in \mathcal{X}_2$ with aspect ratio $Q \in (0, 1]$ is (secularly) stable if and only if $Q > Q_{cr}(2)$. However, in spite of the physical significance of the aspect-ratio Q , the governing relationship between the members $D \in \mathcal{X}_m$, $m \geq 3$, and their aspect-ratios Q_D is very involved and defies prediction of a closed form formula. The situation is changed drastically, as also evident by (3.11) and (3.16), when dealing with Ω instead of Q . In class \mathcal{X}_2 the relationship between Q and Ω is very simple and is determined by (3.13), and, thus,

$$\Omega_{cr}(2) = \frac{3}{16} \quad (Q_{cr}(2) = 3^{-1}). \quad (3.18)$$

To extend the above analysis to more general classes \mathcal{X}_m , $m \geq 3$, and, in particular, in order to obtain their corresponding stability-characteristics we resort to numerical means based on the general theory. This is conducted in Sections 4 and 5.

4. NUMERICAL ALGORITHM

The numerical algorithm consists of two major parts: (1) the "Stationary-State Solver" (SSS) and (2) the "Stability-Analyzer" (SA). The SSS is contained in SA as an integrated component. It is based on a first-order relaxation algorithm, similar to that employed by Pierrehumbert [14] in the two singly-connected regions of vorticity. The present SSS was first developed and carried out in Landau [11], where more details can be found.

In view of (2.1)–(2.2), the stationary state can be determined by solving

$$\psi(z) \equiv \psi_0(z) - \frac{1}{2}\Omega |z|^2 = \text{const.}, \quad z \in C = \partial D, \quad (4.1)$$

where

$$\psi_0(z) = \frac{\omega_0}{2\pi} \int_D \log |\zeta - z| d\sigma(\zeta).$$

Equation (4.1) is rewritten in the following real form, where Fig. 1 may serve as a guide:

$$\begin{aligned} \psi &\equiv \psi_0 - \frac{1}{2}\Omega \rho^2 = c; & c &= \text{const.}, \\ \psi_0(\rho, \Theta) &= \frac{\omega_0}{2\pi} \int_{x_1}^{x_2} H(\rho \cos \Theta - \xi, \rho \sin \Theta - \eta) \Big|_{\eta=-f(\xi)}^{\eta=f(\xi)} d\xi, \\ H(x, y) &= y[2^{-1} \log(x^2 + y^2) - 1] + x \tan^{-1}(y/x), \\ \xi &= \rho(\Theta) \cos \Theta, & 0 &\leq \Theta \leq 2\pi, \\ f(\xi) &= \rho(\Theta) \sin \Theta, & 0 &\leq \Theta \leq \pi. \end{aligned} \quad (4.2)$$

As we are seeking m -fold symmetric states which are also symmetric about the x -axis,

$$\rho(\Theta) = \rho[(2\pi/mM)k + \Theta] = \rho[(2\pi/mM)k - \Theta], \quad k = 0, \dots, mM,$$

and the first equation of (4.2) may be written as an integral over a π/m -sector and a sum over $2m$ sectors. We introduce the dimensionless quantities

$$\begin{aligned} \tilde{\psi}_0 &= \psi_0/(\omega_0 \rho^2(0)), & \tilde{\rho}(\Theta) &= \rho(\Theta)/\rho(0), \\ \tilde{c} &= c/(\omega_0 \rho^2(0)), & \tilde{\Omega} &= \Omega/\omega_0, \end{aligned}$$

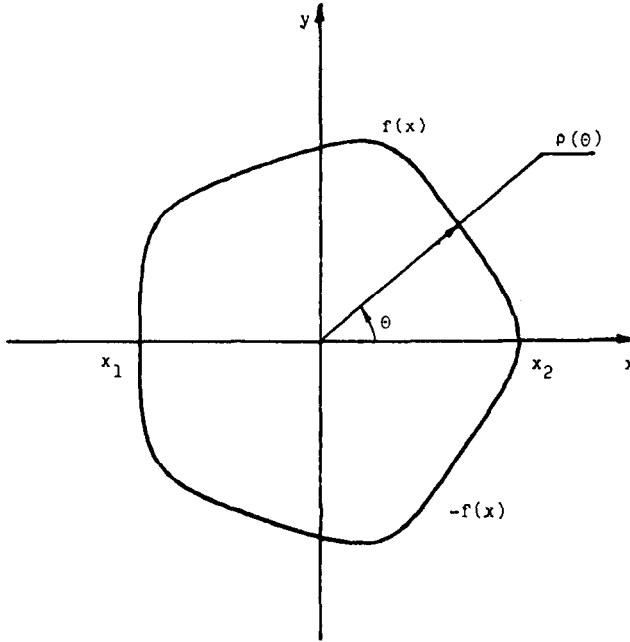


FIG. 1. Rotating singly-connected vortex.

and for convenience we choose

$$\max_{\theta \in [0, 2\pi]} \rho(\theta) = 1 = \rho(0).$$

With these normalized quantities we observe that

$$\begin{aligned} \tilde{c} &= \tilde{\psi}_0(1, 0) - \frac{1}{2}\tilde{\Omega}, \\ \tilde{\Omega} &= 2[\tilde{\psi}_0(1, 0) - \tilde{\psi}_0(\rho_1, \pi/m)]/(1 - \rho_1^2), \quad \rho_1 \equiv \tilde{\rho}(\pi/m). \end{aligned}$$

Moreover, the aspect-ratio Q is now $Q = \rho_1$.

Suppressing the tilde on the normalized quantities, the algorithm aims at finding the zeros of the function

$$E(\theta) \equiv \psi(\theta) - \frac{1}{2}\Omega\rho^2(\theta) - c \quad (\psi(\theta) \equiv \psi_0(\rho(\theta), \theta)) \quad (4.3)$$

over a finite number of θ_j in a sector. Since ψ , Ω and c are functionally dependent on $\rho(\theta)$ by integral expressions, most of the change in $E(\theta)$ is associated with the

change in $\rho(\Theta)$. To minimize the error, we determine the change in radius $\Delta(\Theta)$ by the first-order expansion of $\psi(\Theta)$:

$$\psi_0(\rho(\Theta) + \Delta(\Theta), \Theta) = \psi(\Theta) + \Delta(\Theta) \partial_\rho \psi_0(\rho(\Theta), \Theta)$$

and, thus to a first-order approximation

$$\Delta(\Theta_j) = -E(\Theta_j) / \partial_\rho \psi_0(\rho(\Theta_j), \Theta_j), \quad j = 0, \dots, M.$$

The flow-chart for this SSS is described in Fig. 2.

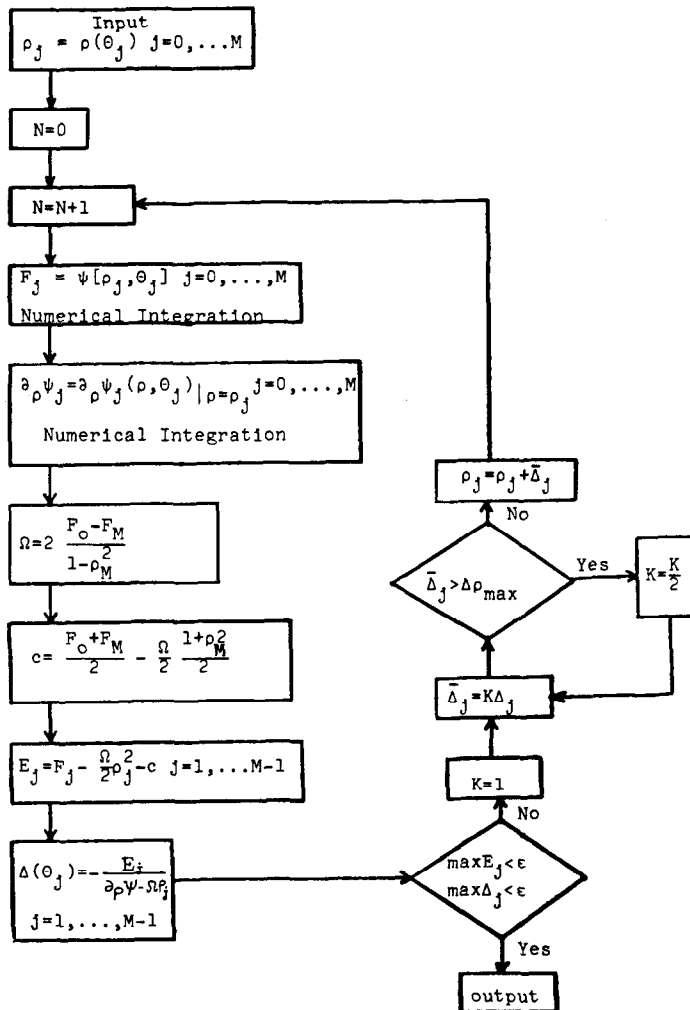


FIG. 2. Flow-chart for the Stationary-State Solver (SSS).

Once a steady state $D \in \mathcal{X}_m$ is computed, the SA is initiated. As a first step in the SA we apply the Theodorsen method (Gaier [6, pp. 61–81], Gutknecht [7, 8] and Henrici [9]) for the determination of the conformal mapping $z = g(\omega)$ which maps $E_\Delta = \{\omega: |\omega| > 1\}$ onto the exterior E_D of D . This mapping is normalized by $g(\infty) = \infty$ and $g'(\infty) = a > 0$, its expansion, therefore, is of the form (2.5). The mapping $z = g(\omega)$ is determined if we can find a continuous function $\Theta(\theta)$ such that

$$\Theta(\theta) = \arg\{g(e^{i\theta})\}, \quad 0 \leq \theta \leq 2\pi. \tag{4.4}$$

equivalent equation

$$\Theta(\theta) = \theta - \frac{1}{2\pi} \int_0^{2\pi} \log \rho[\Theta(t)] \cot \frac{\theta - t}{2} dt, \tag{4.5}$$

where the integral is taken in the principal-value sense. The existence of g is guaranteed by the Riemann-mapping theorem, and, since (4.4) and (4.5) are equivalent, this implies that the nonlinear singular integral equation in (4.5) always has at least one strictly monotone continuous solution. Moreover, it can be shown [6, p. 66; 7] that if $\rho(\Theta)$ satisfies the so called “ ϵ -condition” with $\epsilon < 1$ (a condition which is always fulfilled for the class \mathcal{X}_m), then (4.5) has exactly only one such a solution. After $\Theta(\theta)$ is determined, the coefficients (which now are all real) in (2.5) will be given by

$$b_n = \frac{1}{2\pi a} \int_0^{2\pi} \rho[\Theta(\theta)] \cos[\Theta(\theta) + (n - 1)\theta] d\theta, \quad (n + 1 \equiv 0 \pmod{m}), \tag{4.6}$$

where

$$a = \frac{1}{2\pi} \int_0^{2\pi} \rho[\Theta(\theta)] \cos[\Theta(\theta) - \theta] d\theta. \tag{4.7}$$

We also note that in (4.6), $b_n = 0$ if $n + 1$ is not a multiple of m .

For numerical computations equation (4.5) has to be discretized. This leads to the *discrete Theodorsen equation* [6, p. 85; 7; 8; 9]:

$$\Theta = \theta - K \log \rho(\Theta). \tag{4.8}$$

Here $\theta, \Theta, \log \rho(\Theta)$ are $2N$ -dimensional vectors with components $\theta_k = k\pi/N, \Theta_k$, and $\log \rho(\Theta_k), k = 1, \dots, 2N$, respectively, and $K = (K_{kj})$ is *Wittich’s matrix*:

$$\begin{aligned} K_{kj} &= 0, & \text{if } j - k \text{ even} \\ &= \frac{1}{N} \cot \frac{(k - j)\pi}{2N}, & \text{if } j - k \text{ odd} \quad (k, j = 1, \dots, 2N), \end{aligned} \tag{4.9}$$

where, of course, Θ_k is supposed to approximate $\Theta(\theta_k)$. One shows (cf. Gaier [6, p.

86]) that, again, Eq. (4.8) has exactly one solution and, moreover, the solution can be computed by direct iteration or by variants of Newton's method [9]. These numerical methods are very efficient even for large N (i.e., fine discretization) because the fast Fourier transform can be applied [8]. To implement the Theodorsen method we use the stationary solutions (Θ, ρ) found by the SSS as the initial states

$$\Theta_k^0 = \Theta_k, \quad \rho_k^0 = \rho_k \quad (k = 1, \dots, 2N)$$

for the iteration of (4.8). Next, using

$$\Theta^{l+1} = \theta - K \log \rho(\Theta^l)$$

with K as in (4.9), we calculate Θ_k^{l+1} on the $(1/2m)$ th part of contour C . The rest of the Θ_k^{l+1} can be found by symmetry. Further, we use a piecewise-linear interpolation of the contour C to find ρ_k^{l+1} , and, finally the values of the radii corresponding to the polar angles Θ^{l+1} are corrected by reapplying the SSS.

The coefficients a and b_n of the conformal mapping are computed by a discretized version of Eqs. (4.6)–(4.7), using fast Fourier transform techniques [9]. In this way

$$\hat{a} = \frac{1}{4\pi N} \sum_{k=1}^{2N} \rho_k \cos[\Theta_k - \theta_k]$$

and

$$\hat{b}_n = \frac{1}{4\pi Na} \sum_{k=1}^{2N} \rho_k \cos[\Theta_k + (n-1)\theta_k] \quad (n+1 \equiv 0 \pmod{m}).$$

The fact that $\hat{b}_n = 0$ if $n+1$ is not a multiple of m simplifies the calculations of the Grunsky-coefficients b_{nk} . These coefficients are computed via the \hat{b}_n , the recursive relation (2.15) and the fact that $b_{nk} = 0$ if $n+k$ is not a multiple of m . With these, the real-symmetric Grunsky-matrix $G = (\sqrt{nk} b_{nk})$ is found at once. However, because the sequence $\hat{b} = \{\hat{b}_n\}$ is periodic with period $2N$, it makes no sense to use more than $2N$ terms in the series of (2.5). Consequently, the maximum size of the approximate Grunsky-matrix G will be $(N+1) \times (N+1)$.

It would seem that two errors are committed in the above approximation, namely, (1) the error committed in replacing the exact Fourier-coefficients a and b_n by the approximate Fourier-coefficients \hat{a} and \hat{b}_n , and (2) the error committed in truncating the Fourier series itself. However, as emphasized also in Henrici [9], the present method has the fortunate feature that at least at the sampling points θ_k , these two errors just cancel each other. That is, for $\theta = \theta_k$ the function $\hat{g}(e^{i\theta})$ not only approximates, but actually interpolates the conformal mapping $g(e^{i\theta})$ (cf. Henrici [9] for further details).

We are now in a position to compute the vortex-function $r(\theta)$ as in (2.8) or (2.17). We shall use (2.16)–(2.20). To compute an approximate vortex-function $\hat{r}(\theta)$ at the sampling points θ_k we evaluate the partial derivatives $\partial_x \psi$ and $\partial_y \psi$ in (2.18)–(2.19) using a trapezoidal rule along the indicated contour C . The values of $\dot{x} = dx/d\theta$ and

$\dot{y} = dy/d\theta$ at $\theta = \theta_k$ are determined by taking the real and imaginary part, respectively, of the truncated series

$$\hat{g}(e^{i\theta}) = \frac{d}{d\theta} \hat{g}(e^{i\theta}) = i\hat{a}e^{i\theta} \left(1 - \sum_{n=1}^{2N} (n-1) \hat{b}_n e^{-in\theta} \right), \quad \text{at } \theta = \theta_k.$$

Finally, we obtain $\hat{r}(\theta_k)$ by applying (2.17). As an estimate for the error in calculating $\hat{r}(\theta_k)$ we may use the equation

$$\dot{x}\partial_x \psi + \dot{y}\partial_y \psi = 0, \quad \text{at } \theta = \theta_k, \tag{4.10}$$

reflecting the fact that the boundary C is indeed a streamline for ψ . In our case $r(\theta)$ is m -fold symmetric and, hence, we only have to compute $\hat{r}(\theta_k)$ on the $(1/2m)$ th part of the contour. From (2.16) follows that $r_n = 0$ if n is not a multiple of m and,

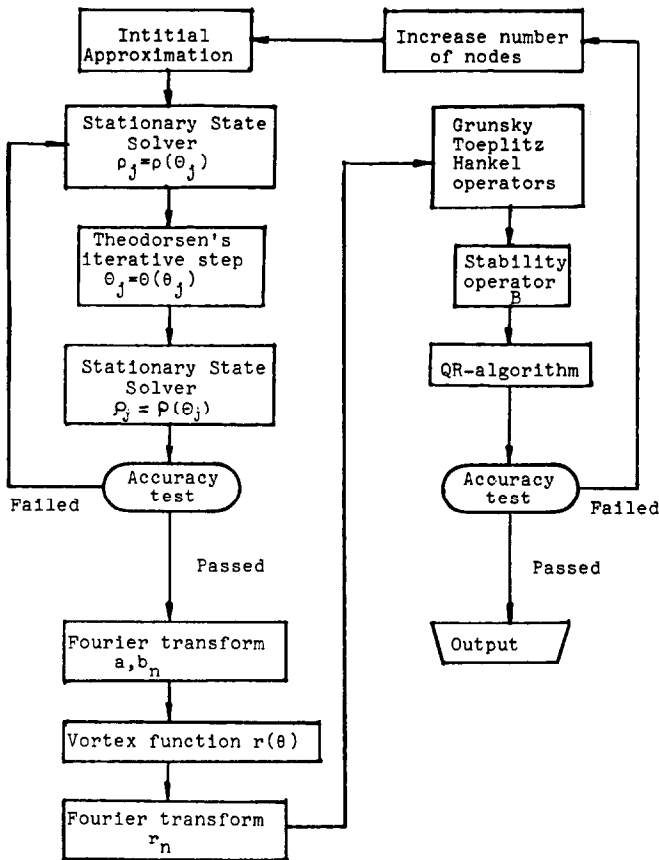


FIG. 3. Flow-chart of the Stability-Analyzer (SA).

moreover, from (2.20) follows that we can again apply the fast Fourier transform to evaluate the non-zero coefficients r_n . With these coefficients we construct the approximate real-symmetric Hankel-matrix $H = (\sqrt{nk} r_{n+k})$ and Toeplitz-matrix $T = (\sqrt{nk} r_{n-k})$. Again, the size of these matrices is $(N+1) \times (N+1)$ and it makes no sense to compute more than $N+1$ coefficients $r_n, n = 0, 1, \dots, N$.

Once the approximate matrices G, H and T are found the approximate stability-matrix B and the companion-matrix J are at once determined via (2.13)–(2.14). We compute the real eigenvalues σ^2 and the corresponding eigenvectors α of the real-symmetric matrix B by employing a QR -algorithm [16] for symmetric matrices, and, we also check, in view of the “Stability-Test” (2), how close the equation $Ja = 0$ is satisfied in the range of stability. This procedure gives $(N+1)$ eigenvalues σ^2 and $(N+1)$ corresponding eigenvectors α . However, the output order of σ^2 and α is, in general, not the natural-modes order. We reorder them in accordance to the “Natural-Modes” (3) rule.

A flow-chart for the SA algorithm is given in Fig. 3. With the above described constructions the entire numerical algorithm for this work is essentially concluded.

5. PROPERTIES OF KELVIN WAVES-NUMERICAL RESULTS

In this section we discuss the properties of the Kelvin class \mathcal{K}_m which are discovered numerically by using the present algorithm. This report complements the

TABLE I.
 m -Fold Symmetric Kelvin Waves \mathcal{K}_m

N	m	Q	Ω	Area	Perimeter	Maximum curvature	Minimum curvature	Error
1	3	0.90	0.33209	2.8192	5.9854	1.5929	0.6925	0.33775×10^{-6}
2	3	0.80	0.32724	2.4799	5.7230	2.6815	0.4300	0.25087×10^{-6}
3	3	0.70	0.31787	2.1171	5.4967	5.2127	0.2378	0.11437×10^{-6}
4	3	0.60	0.30326	1.6989	5.2884	22.2603	0.1707	0.10966×10^{-8}
5	3	0.52	0.28221	1.4225	5.2080	236.2933	-19.2714	0.97648×10^{-3}
6	4	0.90	0.37300	2.8112	6.0060	2.1956	0.4303	0.17131×10^{-6}
7	4	0.80	0.36583	2.4428	5.8058	5.3962	0.0528	0.83094×10^{-7}
8	4	0.70	0.35398	1.9876	5.8228	91.7892	-0.0612	0.34692×10^{-6}
9	4	0.67	0.35122	1.9005	5.6693	95.7830	-0.7994	0.88179×10^{-3}
10	5	0.90	0.39729	2.8028	6.0345	3.1495	0.1357	0.11401×10^{-6}
11	5	0.80	0.38793	2.3971	5.9199	14.4136	-0.2798	0.88289×10^{-6}
12	5	0.75	0.38293	2.1578	5.9195	115.4890	-0.6259	0.25398×10^{-3}
13	6	0.90	0.41326	2.7940	6.0713	4.6308	-0.1723	0.66011×10^{-7}
14	6	0.87	0.41068	2.6740	6.0496	7.5071	-0.3685	0.84005×10^{-6}
15	6	0.80	0.40419	2.3282	6.1128	17.8749	-0.5069	0.13039×10^{-6}

TABLE II
 Fourier Coefficients ρ_n of $\rho = \rho(\theta)$ for class \mathcal{A}_m , $\rho(\theta) = \sum_{n=0}^{\infty} \rho_n \cos(nm\theta)$
 (Sequential Numbers N Correspond to Those of Table I)

N/n	0	1	2	3	4	5	6	7	8	9	10
1	0.9496	0.0249	0.0013	0.0001	0.0000	0.0000	0.0000	0.0000	0.0000	0.0000	0.0000
2	0.8895	0.0490	0.0062	0.0011	0.0001	0.0000	0.0001	0.0000	0.0000	0.0000	0.0000
3	0.8192	0.0701	0.0149	0.0045	0.0014	0.0005	0.0001	0.0000	0.0000	0.0000	0.0000
4	0.7304	0.0820	0.0257	0.0117	0.0060	0.0036	0.0022	0.0015	0.0010	0.0006	0.0004
5	0.6618	0.0891	0.0289	0.0147	0.0082	0.0055	0.0037	0.0029	0.0022	0.0018	0.0015
6	0.9481	0.0248	0.0021	0.0003	0.0001	0.0000	0.0000	0.0000	0.0000	0.0000	0.0001
7	0.8831	0.0474	0.0089	0.0025	0.0005	0.0001	0.0000	0.0000	0.0002	0.0002	0.0000
8	0.7949	0.0590	0.0180	0.0088	0.0048	0.0030	0.0021	0.0015	0.0015	0.0012	0.0008
9	0.7749	0.0636	0.0178	0.0089	0.0050	0.0033	0.0023	0.0017	0.0012	0.0010	0.0007
10	0.9468	0.0246	0.0026	0.0005	0.0000	0.0000	0.0000	0.0000	0.0000	0.0000	0.0000
11	0.8738	0.0443	0.0113	0.0043	0.0019	0.0010	0.0005	0.0003	0.0002	0.0001	0.0001
12	0.8284	0.0478	0.0138	0.0067	0.0038	0.0025	0.0017	0.0013	0.0010	0.0008	0.0006
13	0.9453	0.0243	0.0033	0.0007	0.0001	0.0000	0.0000	0.0000	0.0000	0.0000	0.0000
14	0.9241	0.0307	0.0058	0.0017	0.0005	0.0002	0.0001	0.0000	0.0000	0.0000	0.0000
15	0.8617	0.0377	0.0111	0.0052	0.0029	0.0018	0.0012	0.0009	0.0007	0.0005	0.0005

preliminary report in Section 3. The latter, however, may serve as a guide and a motivation for the numerical findings that we discuss here.

The stationary states of the class \mathcal{K}_m , $2 \leq m \leq 6$, are computed via the SSS. The numerical results are presented in Tables I–II and Figs. 4, 5. The classical elliptic case of $m = 2$, however, is not reported explicitly as it has already been described in (3.4)–(3.18). Table I, for $3 \leq m \leq 6$, gives Ω , Q and the characteristics of the contour of $D \in \mathcal{K}_m$. This includes area, perimeter, maximum-curvature and minimum-curvature. It also provides the maximum of the error $E(\theta)$ of (4.3). Table II contains the first ten modes of the Fourier-cosine representation that allows one to reconstruct the contour to four significant figures. The present steady states are also in agreement with the computations of Burbea [3] which are based on asymptotic expansions of conformal mappings. The theoretical range of existence $\Omega_{m-1} < \Omega \leq \Omega_m$ in (3.11) is recovered to four significant figures. Table I indicates that the area and the perimeter of the vortex are directly related to its aspect-ratio Q , a fact which may also be

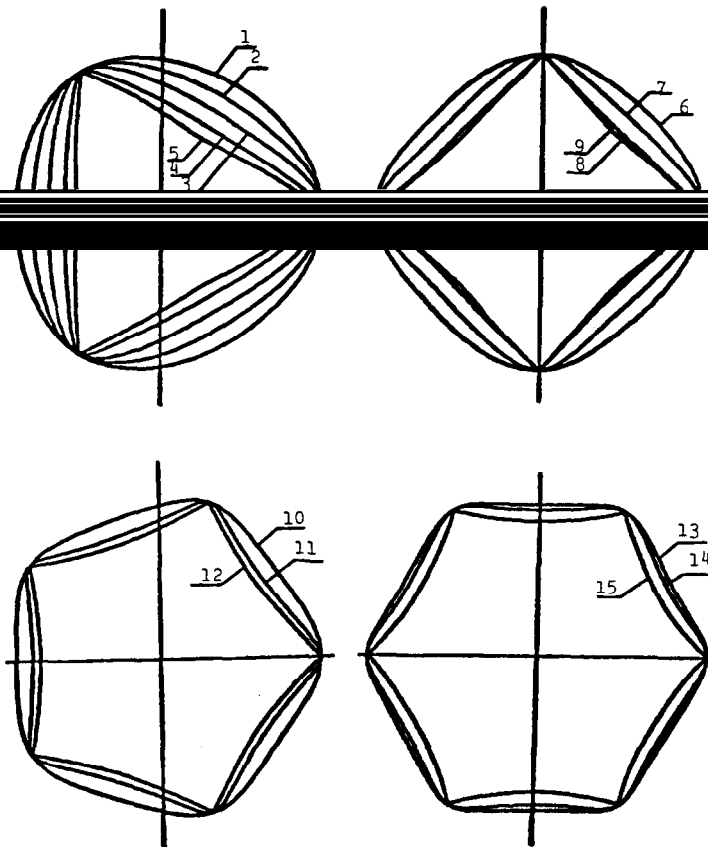


FIG. 4. m -fold symmetric Kelvin waves \mathcal{K}_m (sequential numbers $N = 1, \dots, 15$, correspond to those of Table I).

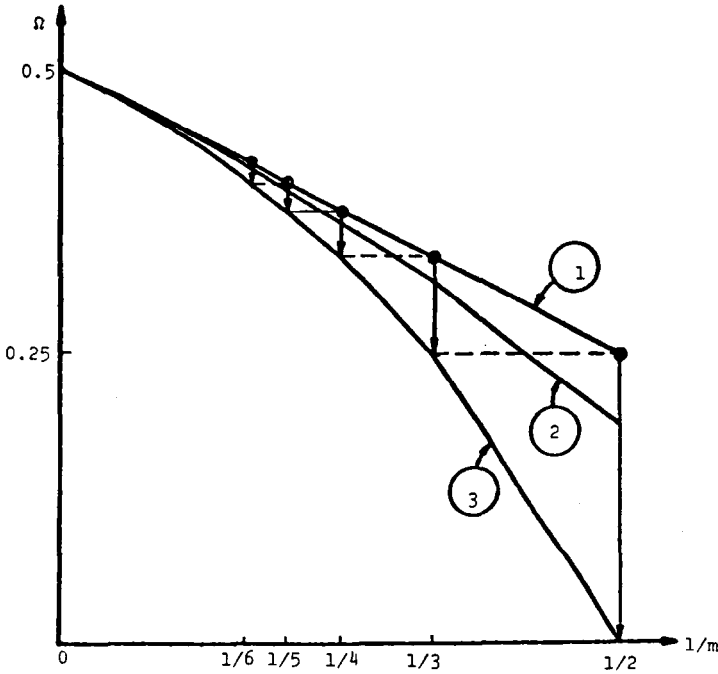


FIG. 5. Existence and stability diagram for the class \mathcal{X}_m . (1) Upper bound for existence and stability of solutions ($\Omega_m = (1/2)(m - 1)/m$). (2) Lower bound for stability of solutions ($\Omega_{cr}(m) = (1/8)[3(m - 1)/m + (m - 2)/(m - 1)]$). (3) Lower bound for existence of solutions ($\Omega_{m-1} = (1/2)(m - 2)/(m - 1)$).

predicted via analytical means. On the other hand, the maximum-curvature of the contour is oppositely related to the aspect-ratio, indicating the formation of cusps when $Q = 2\Omega_{m-1} = (m - 2)/(m - 1)$. This suggests the number $2\Omega_{m-1}$ as the supremum for the allowable aspect-ratio of the class \mathcal{X}_m . Indeed, on also using (3.11), the ranges of Q and Ω in the class \mathcal{X}_m are

$$2\Omega_{m-1} < Q \leq 1, \quad \Omega_{m-1} < \Omega \leq \Omega_m. \tag{5.1}$$

Moreover, Q and Ω are functionally related by $\Omega = f_m(Q)$ with the f_m being a positive smooth function which is monotonically increasing on the interval $[2\Omega_{m-1}, 1]$. Also, f_m maps $[2\Omega_{m-1}, 1]$ onto $[\Omega_{m-1}, \Omega_m]$ with

$$f_m(2\Omega_{m-1}) = \Omega_{m-1}, \quad f_m(1) = \Omega_m. \tag{5.2}$$

This relationship between the endpoints corresponds to the bifurcation of the circle-solutions as in (3.9) (cf. Burbea [1]). A closed-form formula for $f_m(Q)$, $m \geq 3$, is not available.

We also note that by (5.1) the supremum of Ω for all the classes \mathcal{X}_m is $1/2$ (see

Fig. 5) which corresponds to \mathcal{K}_∞ . However, the class $\mathcal{K}_\infty = \lim_{m \rightarrow \infty} \mathcal{K}_m$ would have an indeterminate meaning.

As for the application of Theodorsen's method of the found states of \mathcal{K}_m , we first tested it to the ellipses of \mathcal{K}_2 . Computations with different ellipses have shown the quick convergence of the iterative-procedure (20–60 iterations) for solving the discrete Theodorsen equation. Using 100 nodal points on one quarter of the ellipses we were able to recover the correspondance function $\Theta(\theta)$ up to six significant figures. Also we computed the eigenvalues of the stability-operator B with an accuracy of up to three significant figures.

Similar results are obtained for the class \mathcal{K}_m , $3 \leq m \leq 6$. Again, to achieve the three significant figures accuracy, 100 nodal points per $(1/2m)$ th part of the contour are needed. We compute the coefficients for the conformal mapping of a $D \in \mathcal{K}_m$ by using Theodorsen's method, and, compare them with the results of Burbea [3]. In Burbea [3], few of these coefficients were computed analytically by using methods of asymptotic expansions. The comparison shows the agreement in six significant figures. In all computed states, the test in (4.10) has been satisfied up to five significant figures while the test $J\alpha = 0$ of the "Stability-Test" (2), within the range of stability, is satisfied up to three–four significant figures.

Figure 6 shows the examples of the first six natural harmonics $F_n(\theta)$, $1 \leq n \leq 6$, of

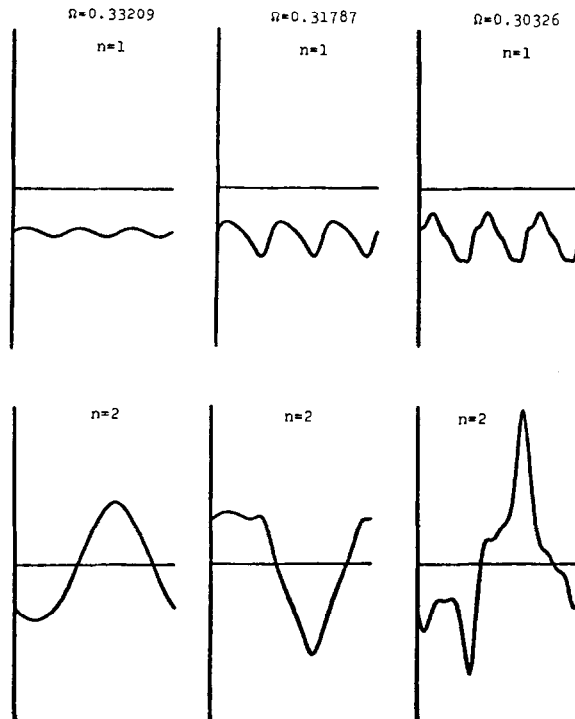


FIG. 6. Natural harmonics $F_n(\theta)$ of class \mathcal{K}_3 (based on "Natural-Modes" (3) rule).

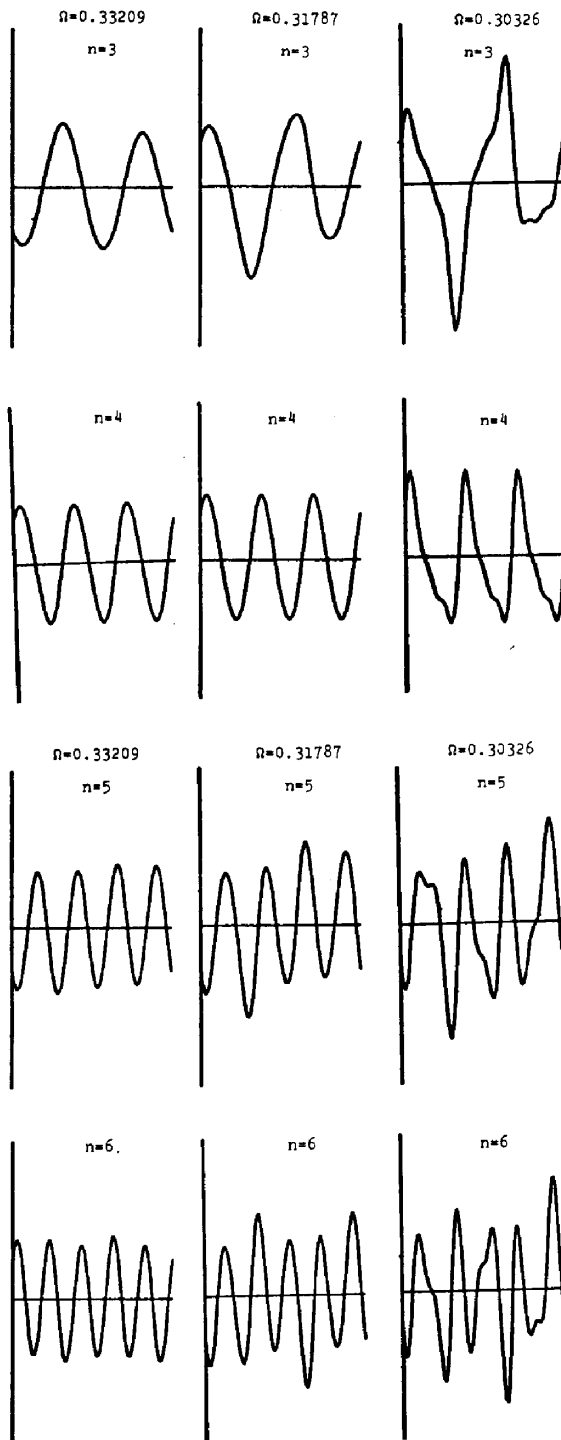


FIG. 6—Continued.

TABLE III
 Natural n -Eigenvalues of the Stability-Operator B for Classes \mathcal{K}_m ($m = 3, 4$)

n/Ω	$m = 3$				$m = 4$		
	0.33209	0.032724	0.31787	0.30326	0.37300	0.36583	0.35398
1	0.11029	0.10713	0.10112	0.09218	0.13913	0.13384	0.12532
2	0.02706	0.02528	0.02145	0.01493	0.06145	0.05393	0.04348
3	-0.00000	-0.00000	-0.00001	0.00002	0.01483	0.01025	0.00378
4	0.02642	0.02032	0.00888	-0.00509	-0.00000	-0.00001	-0.00002
5	0.10771	0.09216	0.06134	-0.00214	0.01247	0.00217	-0.00368
6	0.24386	0.21559	0.13314	0.02447	0.05491	0.01758	-0.00747
7	0.43490	0.39068	0.29955	0.14720	0.12684	0.06753	-0.00725
8	0.68080	0.61740	0.48573	0.30630	0.23573	0.15824	0.04355

the “Natural-Modes” (3) rule for 3-fold symmetric states $D \in \mathcal{K}_3$ with the different angular velocities $\Omega = 0.33209, 0.32724, 0.30326$. The eigenvalues of the stability-operator B are given in Table III. The dispersion-diagram $\sigma_n^2 = \sigma_n^2(\Omega)$ as determined by the “Dispersion-Relation” (4) rule for $2 \leq m \leq 4$ is shown in Fig. 7, where the solid lines represent computed eigenvalues of the operator B while the dashed lines illustrate our prediction of the behaviour of these eigenvalues in the range of non-stability. The prediction is based on the computed results for the elliptic state and on the fact that higher harmonics cannot pass the point of infinite curvature. Consequently, using the notation of (3.2)

$$\lambda_m(n; \Omega) \equiv \sigma_n^2(\Omega), \quad m \geq 2,$$

we have

$$\lim_{\Omega \rightarrow \Omega_{m-1}} [\partial_\Omega \lambda_m(n; \Omega)] = 0, \quad n = m - 1, m, m + 1, \dots$$

A further analysis of the dispersion-digram (Fig. 7 and Table III) leads to the following stability-characteristics of the class \mathcal{K}_m :

(1) For any $m \geq 2$, the natural m -eigenvalue $\lambda_m(m; \Omega) = \sigma_m^2(\Omega)$ is always zero on the range of existence $\Omega_{m-1} < \Omega \leq \Omega_{m-1}$, within four significant figures accuracy. This means that the states of \mathcal{K}_m are never stable with respect to the m -mode. The special case with $m = 2$ is exhibited in (3.17).

(2) The critical value of stability of the class \mathcal{K}_m in terms of the angular velocity is

$$\Omega_{cr}(m) = \frac{1}{8} \left(3 \frac{m-1}{m} + \frac{m-2}{m-1} \right), \quad m \geq 2,$$

a formula coinciding with (3.18) when $m = 2$ (see also Love [13]). This formula is

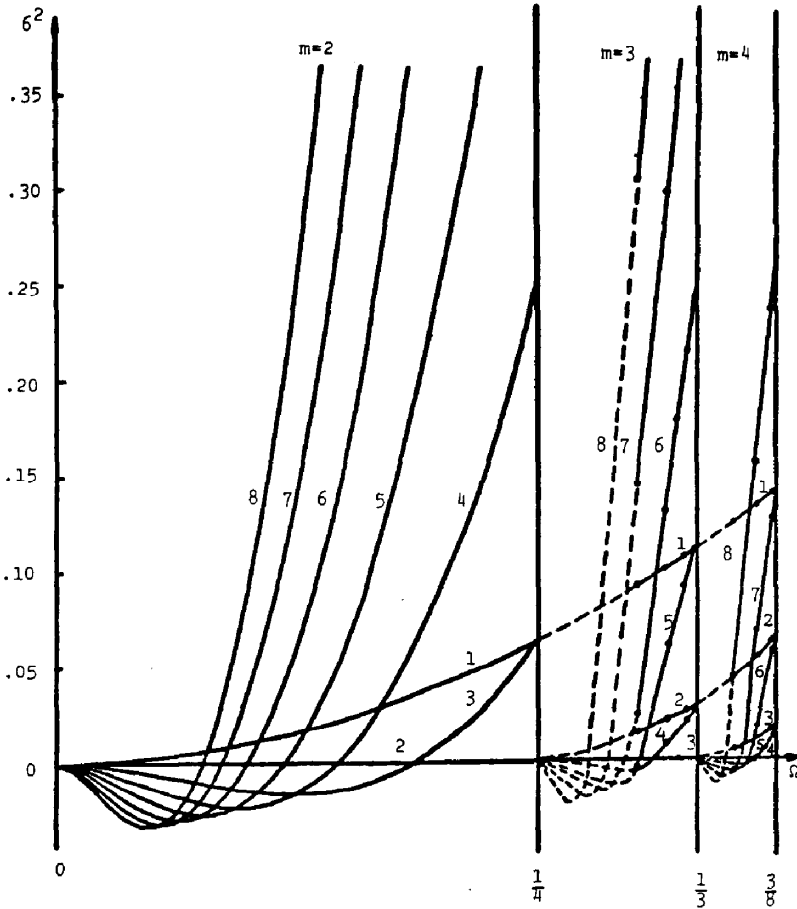


FIG. 7. Dispersion diagram for classes \mathcal{K}_m ($m = 2, 3, 4$)
 (the curve number n , $n = 1, \dots, 8$, corresponds to the n -natural eigenvalue $\lambda_n(n; \Omega) = \sigma_n^2(\Omega)$).

validated up to three significant figures. With the notation of (5.1)–(5.2) we have $\Omega = f_m(Q)$ and, therefore,

$$\frac{1}{4}(3\Omega_m + \Omega_{m-1}) = \Omega_{cr}(m) = f_m[Q_{cr}(m)].$$

The uniquely determined critical values $Q_{cr}(m)$ and $\Omega_{cr}(m)$ are computed numerically and are given in Table IV. We were not able to suggest a closed-form expression for the value of $Q_{cr}(m)$, $m \geq 3$.

(3) For any number Ω (or Q) satisfying (5.1) there exists a state $D \in \mathcal{K}_m$ which is unique up to rotation, magnification and reflection, such that Ω is its angular velocity (or Q is its aspect-ratio). Moreover, the state D is (secularly) stable if and only if $\Omega > \Omega_{cr}(m)$ or $Q > Q_{cr}(m)$ (see Fig. 5).

TABLE IV
Critical Values of Aspect Ratios and
Angular Velocities for Class \mathcal{K}_m

m	$Q_{cr}(m)$	$\Omega_{cr}(m)$
2	0.3333	0.1875
3	0.6654	0.3122
4	0.7845	0.3641
5	0.8532	0.3933
6	0.8911	0.4120

(4) According to (1) and (3) the states of \mathcal{K}_m are (secularly) stable for $\Omega > \Omega_{cr}(m)$ and they are never stable with respect to the m -mode. This phenomenon is well understood even in the classical literature (see, for example, Love [13] for the case of $m = 2$). Indeed, the perturbation of a stationary state $D \in \mathcal{K}_m$ by the natural m -harmonic corresponds to a generation of another stationary state $D_\epsilon \in \mathcal{K}_m$ with an angular velocity Ω_ϵ slightly different from the older angular velocity Ω of D , and the disturbed state D_ϵ tends in a very long, but finite, time to become finitely different from the undisturbed state D . This kind of perturbation is labeled as “secular”. However, any other perturbation orthogonal to the secular m -harmonic in $L_2(D)$ is oscillatory in character, provided $\Omega_{cr}(m) < \Omega \leq \Omega_m$. When $\Omega_{m-1} < \Omega \leq \Omega_{cr}(m)$ the state D becomes unstable and even a very small disturbance causes the development of “tentacles” (see also Landau [11]).

(5) The motion of any $D \in \mathcal{K}_m$ is stable for any disturbance whose natural harmonics are of order lower than m . The $(m + 1)$ -natural harmonic is always the first one that causes the motion to become unstable.

(6) In the limiting case of $\Omega = \Omega_m$, i.e., when $D \in \mathcal{K}_m$ becomes the circle solution, the natural $(m + n)$ -eigenvalue is equal to the natural $(m - n)$ -eigenvalue for

$$\lambda_m(m + n; \Omega_m) = \lambda_m(m - n; \Omega_m) = \left(\frac{n}{2m}\right)^2; \quad 1 \leq n \leq m - 1.$$

(7) As a function on the interval $(0, 1/2)$, $\sigma_n^2(\Omega)$ for $n \geq 2$ has exactly $(n - 2)$ jumps at the points $\Omega = \Omega_k$ with

$$\Omega_k = (k - 1)/2k, \quad k = 2, \dots, n - 1.$$

It can be negative on parts of the intervals

$$\Omega_{k-1} < \Omega < \Omega_k, \quad k = 2, \dots, n - 1.$$

On the $(n - 1)$ -interval

$$\Omega_{n-2} < \Omega < \Omega_{n-1},$$

$\sigma_n^2(\Omega)$ crosses the Ω -axis at three quarters of this interval. On the next interval $\sigma_n^2(\Omega) = 0$ and becomes positive and continuous for

$$\Omega_n < \Omega < 1/2.$$

(8) For disturbances associated with the $n = 1$ mode, all states $D \in \mathcal{X}_m$, for any $m \geq 2$, are stable. This perturbation corresponds to a slight displacement of the steady vortex D without change of form and the perturbed vortex tends to oscillate about its original position as a mean. The angular velocity of these oscillations is the same as the angular velocity of the vortex, that is

$$\sigma_1(\Omega) = \pm \Omega \quad (\sigma_1^2(\Omega) = \lambda_m(1: \Omega)).$$

Again, the special case of $m = 2$ is exhibited in (3.17).

Finally, we discuss the behaviour of the natural n -eigenvalue $\lambda_m(n: \Omega) = \sigma_n^2(\Omega)$ of the stability-operator B of the state $D \in \mathcal{X}_m$ as a function of $n \geq 1$. In order to

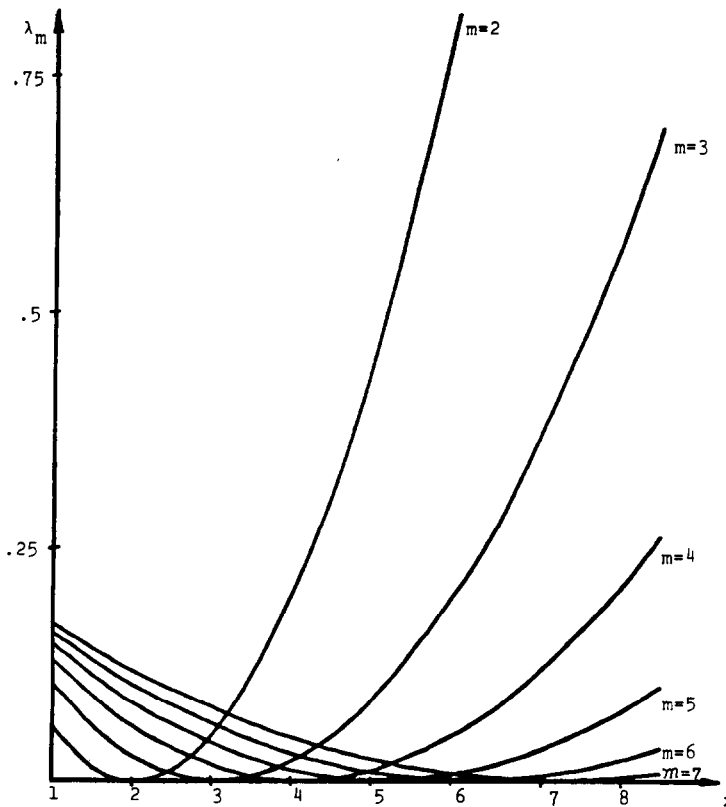


FIG. 8. Natural eigenvalue diagram (circle-solution). $\lambda_m(x: \Omega_m) = \frac{1}{4}(x/m - 1)^2, x \geq 1$.

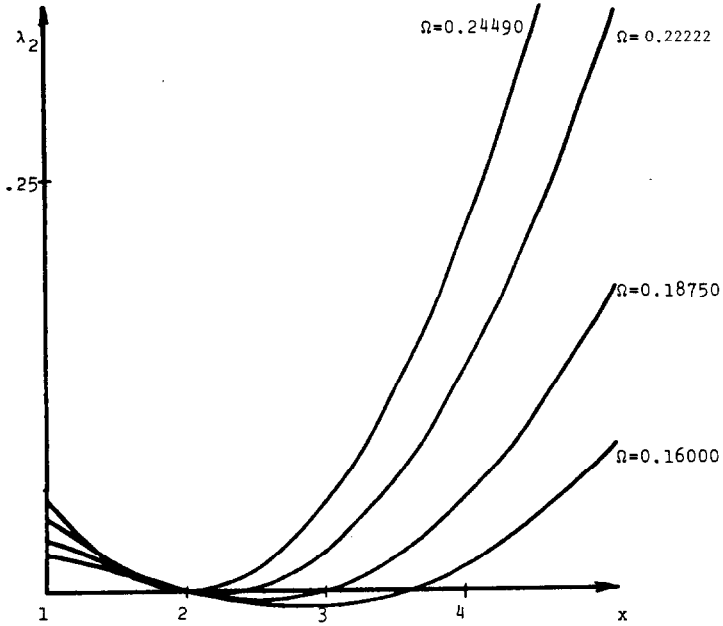


FIG. 9. Natural eigenvalue diagram for class \mathcal{S}_2 (elliptic-solution).
 $\lambda_2(x; \Omega) = \frac{1}{4}\{(1 - 2\Omega x)^2 - (1 - 4\Omega)^x\}$, $x \geq 1$.

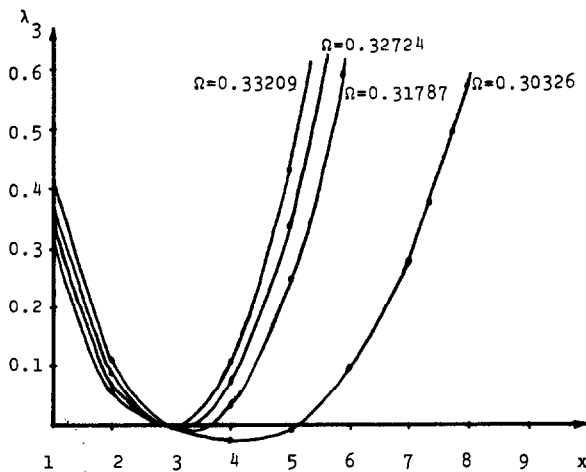


FIG. 10. Natural eigenvalue diagram for class \mathcal{S}_3 , $\lambda_3 = \lambda_3(x; \Omega)$, $x \geq 1$.

emphasize this behaviour we replace the discrete variable n by a continuous variable $x \in [1, \infty)$ and consider the function

$$\lambda_m(x) \equiv \lambda_m(x; \Omega), \quad x \in [1, \infty)$$

where the bifurcation parameter Ω is restricted to the interval of (5.1)

$$\Omega_{m-1} < \Omega \leq \Omega_m.$$

This function possesses the following properties (see Fig. 8–10):

- (1) $\lambda_m(x)$ is concave-up with a single minimum at $m \leq x_{\min} < \infty$;
- (2) $\lambda_m(x) > 0$ for $1 \leq x < m$, $\lambda_m(m) = 0$ and $x_{\min} = m$ if and only if $\Omega = \Omega_m$;
- (3) $\lambda_m(x)$, for $\Omega_{m-1} < \Omega < \Omega_m$, vanishes at $x = m$ and at $x = x_0$, where $m < x_{\min} < x_0$. Moreover, $x_0 < m + 1$, $x_0 = m + 1$ or $x_0 > m + 1$ if and only if $\Omega > \Omega_{cr}(m)$, $\Omega = \Omega_{cr}(m)$ or $\Omega < \Omega_{cr}(m)$, respectively.

Again, the above listed properties of $\lambda_m(x)$ determine $\Omega_{cr}(m)$ and all the other stability characteristics of the class \mathcal{K}_m . The present numerical results are in a full agreement with the analytical results concerning the circle solutions and the class \mathcal{K}_2 exhibited in Section 3.

The above dispersion-diagrams and in particular those of Fig. 7 contain further additional information than the one we have described here. However, because of the clarity of the diagrams and the scope of the present paper we regard the description of the stability-characteristics of the class \mathcal{K}_m as essentially concluded.

ACKNOWLEDGMENTS

We wish to acknowledge stimulating discussions with N. J. Zabusky, University of Pittsburgh, on the present topics. We also used the computational facilities (DEC 10) of the University of Pittsburgh in carrying out the present numerical work.

REFERENCES

1. J. BURBEA, in "Proceedings Nonlinear Evol. Equat. and Dynamical Systems, Lecce 1979," Springer Lecture Notes in Physics 120 (1980), 276–298.
2. J. BURBEA, in "Proceedings Nonlinear Phenomena in Math. Sci., Arlington," Academic Press, New York/London, 1981.
3. J. BURBEA, in "Proceedings Nonlinear Analysis, St. Johns 1981," Academic Press, New York/London, 1982.
4. J. BURBEA, to appear.
5. G. S. DEEM AND N. J. ZABUSKY, *Phys. Rev. Lett.* **40** (1978), 859–862.
6. D. GAIER, "Konstruktive Methoden der Konformen Abbildung," Springer-Verlag, Berlin, 1964.
7. M. H. GUTKNECHT, Existence of a solution to the discrete Theodorsen equation for conformal mappings, *Math. Comp.* **31** (1977), 478–480.
8. M. H. GUTKNECHT, "Solving Theodorsen's Integral Equation for Conformal Maps with the Fast Fourier Transform, I," ETH Research Report 79–02, 1979.

9. P. HENRICI, *SIAM Rev.* **21** (1979), 481–527.
10. H. LAMB, “Hydrodynamics,” Dover, New York, 1932.
11. M. LANDAU, “The Structure and Stability of Finite Area Vortex Regions of the Two Dimensional Euler Equations,” dissertation, Univ. of Pittsburgh, 1981.
12. M. LANDAU AND N. J. ZABUSKY, to appear.
13. A. E. H. LOVE, *Proc. London Math. Soc. (1)* **25** (1893), 18–42.
14. R. T. PIERREHUMBERT, *J. Fluid Mech.* **99** (1980), 129.
15. P. G. SAFFMAN AND R. SZETO, *Stud. Appl. Math.*, in press.
16. J. H. WILKINSON, “The Algebraic Eigenvalue Problem,” Oxford Univ. Press (Clarendon), Oxford, 1965.